PHYSICAL REVIEW D **72,** 034006 (2005)

Even- and odd-parity charmed meson masses in heavy hadron chiral perturbation theory

Thomas Mehen[1,2,*] and Roxanne P. Springer[1,†]

[1]*Department of Physics, Duke University, Durham, North Carolina 27708, USA*
[2]*Jefferson Laboratory, 12000 Jefferson Avenue, Newport News, Virginia 23606, USA*
(Received 20 April 2005; published 9 August 2005)

We derive mass formulas for the ground state, $J^P = 0^-$ and 1^-, and first excited even-parity, $J^P = 0^+$ and 1^+, charmed mesons including one-loop chiral corrections and $O(1/m_c)$ counterterms in heavy hadron chiral perturbation theory. We show that including these counterterms is critical for fitting the current data. We find that certain parameter relations in the parity doubling model are not renormalized at one-loop, providing a natural explanation for the observed equality of the hyperfine splittings of ground state and excited doublets.

DOI: 10.1103/PhysRevD.72.034006 PACS numbers: 12.39.Fe, 12.39.Hg

I. INTRODUCTION

Excited charmed mesons with angular momentum and parity $J^P = 0^+$ and 1^+ have been observed in several experiments. The masses of the $J^P = 0^+$ and 1^+ charmed strange mesons, $D_s(2317)$ and $D_s(2460)$ [1,2], are below threshold for decays into ground state charmed mesons and kaons. The only strong decay modes are via isospin-violating π^0 emission, making the states quite narrow ($\Gamma <$ 5.5 MeV). Other experiments [3–5] claim to observe the nonstrange $J^P = 0^+$ and 1^+ states. These states can decay to the ground states by S-wave pion emission and therefore are quite broad ($\Gamma \sim 300$ MeV).

The spectrum of the $J^P = 0^+$ and 1^+ charmed mesons presents a number of puzzles for theory. Before their discovery, quark model and lattice calculations predicted that the masses of the $J^P = 0^+$ and 1^+ charmed strange mesons would be significantly higher than observed [6–10]. Further, the hyperfine splittings of all ground state charmed mesons and the hyperfine splitting of the $D_s(2317)$ and $D_s(2460)$ are all equal to within 2%. This is surprising because there is no obvious symmetry of quantum chromodynamics (QCD) which predicts these equalities. Finally, the $SU(3)$ splittings of the $J^P = 0^+$ and 1^+ charmed mesons are much smaller than theoretical expectations.

In the heavy quark limit, the coupling of the heavy quark spin to the light degrees of freedom in the heavy meson vanishes and the angular momentum and parity of the light degrees of freedom, j^p, can be used to classify heavy meson states. The spectrum consists of degenerate heavy meson doublets with definite j^p. The $J^P = 0^-$ and 1^- heavy mesons are members of the $j^p = \frac{1}{2}^-$ ground state doublet. The lowest lying excited states, the $J^P = 0^+$ and 1^+ heavy mesons, are members of the $j^p = \frac{1}{2}^+$ doublet. There is also an excited doublet of heavy mesons with $j^p = \frac{3}{2}^+$, whose members have $J^P = 1^+$ and 2^+. The $j^p = \frac{3}{2}^+$ mesons decay to the ground state by D-wave pion emission, typically have widths $\Gamma \sim 20$ MeV, and therefore have well-measured masses. The hyperfine splittings for all of these heavy quark doublets are suppressed by $1/m_Q$, where m_Q is the heavy quark mass.

The experimental data on the masses of the known charmed mesons is summarized in Table I. The lowest lying flavor $SU(3)$ antitriplets are $J^P = 0^-$ ($c\bar{u}$, $c\bar{d}$, $c\bar{s}$) $\sim$ (D^0, D^+, D_s^+) and $J^P = 1^-$ (D^{*0}, D^{*+},D_s^{*+}). The first excited states are $J^P = 0^+$ (D_0^0, D_0^+,D_{0s}^+) and $J^P = 1^+$ ($D_1^{0\prime}$, $D_1^{+\prime}$, $D_{1s}^{+\prime}$). The members of the $j^p = \frac{3}{2}^+$ doublet are $J^P = 1^+$ (D_1^0, D_1^+, D_{1s}^+) and $J^P = 2^+$ (D_2^0, D_2^+, D_{2s}^+). Not shown is a narrow charmed strange meson, $D_s^+(2632)$, recently observed by the SELEX collaboration [11]. The spin and parity of this meson and its place in the charmed meson spectrum is currently unknown. For all mesons except the nonstrange $j^p = \frac{1}{2}^+$ doublet, we use numbers from the Particle Data Group [12]. For nonstrange $j^p = \frac{1}{2}^+$ mesons, we use the Belle [4] measurement of the D_0^0 mass and average the CLEO [3] and Belle [4] measurements of the D_1^0 mass.[1]

As stated earlier, the hyperfine splittings of the $j^p = \frac{1}{2}^-$ and $j^p = \frac{1}{2}^+$ doublets are nearly equal. The known hyperfine splittings of the $j^p = \frac{1}{2}^-$ and $j^p = \frac{1}{2}^+$ charmed mesons are:

*Electronic address: mehen@phy.duke.edu
†Electronic address: rps@phy.duke.edu

[1]The FOCUS collaboration reports structures in excess of background in the $D^+\pi^-$ and $D^0\pi^+$ invariant mass spectra which could be interpreted as scalar resonances [5]. However, if these resonances exist their masses are 99 MeV higher than the Belle measurement and 80 MeV higher than the mass of the D_{s0}^+. It is implausible that such resonances are related to the D_{s0}^+ by $SU(3)$ symmetry so we do not use this data to determine the $J^P = 0^+$ nonstrange meson masses.

1550-7998/2005/72(3)/034006(12)$23.00

TABLE I. The spectrum of charmed mesons. j^p is the angular momentum and parity of the light degrees of freedom. J^P is the angular momentum and parity of the meson.

j^p	J^P	$c\bar{u}$		$c\bar{d}$		$c\bar{s}$	
		name	M(MeV)	name	M(MeV)	name	M(MeV)
$3/2^+$	2^+	D_2^0	2458.9 ± 2.0	D_2^+	2459 ± 4	D_{s2}^+	2572.4 ± 1.5
$3/2^+$	1^+	D_1^0	2422.2 ± 1.8	D_1^+	2427 ± 5	D_{s1}^+	2535.4 ± 0.6
$1/2^+$	1^+	$D_1^{0\prime}$	2438 ± 31	$\cdots$	$\cdots$	$D_{s1}^{+\prime}$	2459.3 ± 1.3
$1/2^+$	0^+	D_0^0	2308 ± 36	$\cdots$	$\cdots$	D_{s0}^+	2317.4 ± 0.9
$1/2^-$	1^-	D^{*0}	2006.7 ± 0.5	D^{*+}	2010.0 ± 0.5	D_s^{*+}	2112.1 ± 0.7
$1/2^-$	0^-	D^0	1864.6 ± 0.5	D^+	1869.4 ± 0.5	D_s^+	1968.3 ± 0.5

$$\begin{aligned} m_{D^{*0}} - m_{D^0} &= 142.1 \pm 0.07\ \text{MeV} \\ m_{D^{*+}} - m_{D^+} &= 140.6 \pm 0.1\ \text{MeV} \\ m_{D_s^{*+}} - m_{D_s^+} &= 143.8 \pm 0.4\ \text{MeV} \\ m_{D_{s1}^{+\prime}} - m_{D_{s0}^+} &= 141.9 \pm 1.6\ \text{MeV} \\ m_{D_1^{0\prime}} - m_{D_0^0} &= 130 \pm 48\ \text{MeV}. \end{aligned} \tag{1}$$

Here, the first three numbers are the hyperfine splittings quoted by the Particle Data Group [12]. The last two numbers are obtained by taking the difference of the masses in Table I. The error in the last two lines of Eq. (1) is obtained by adding the errors in the individual masses in quadrature. All four hyperfine splittings which have been measured accurately are ≈ 142 MeV to within 2 MeV or less. Hyperfine splittings in different heavy quark doublets are unrelated by heavy quark symmetry. For example, the hyperfine splitting for $j^p = \frac{3}{2}^+$ doublets is ~ 40 MeV, which differs significantly from the $j^p = \frac{1}{2}^-$ and $\frac{1}{2}^+$ hyperfine splittings. In the $SU(3)$ limit, the hyperfine splittings of nonstrange and strange ground state mesons are the same. That this $SU(3)$ prediction holds to within 2% is surprising given the typical size of $SU(3)$ breaking effects in QCD.

Another puzzling feature of the spectrum is the pattern of $SU(3)$ violation in the splittings within the even-parity doublets. Finite light quark (m_u, m_d, and m_s) masses and electromagnetic effects cause flavor-splitting among the mesons. The isospin splitting seen in the charmed meson mass spectrum is of expected size, but the splitting between the strange and nonstrange sector is unexpected. The mass difference between strange and nonstrange mesons whose other quantum numbers are identical is expected to be ~ 100 MeV. For the ground state charmed mesons this is indeed the case. For the excited states, however, the $SU(3)$ breaking is

$$\begin{aligned} m_{D_{s1}^{+\prime}} - m_{D_1^{0\prime}} &= 21 \pm 31\ \text{MeV} \\ m_{D_{s0}^+} - m_{D_0^0} &= 9 \pm 36\ \text{MeV}. \end{aligned} \tag{2}$$

Even allowing for the large errors due to the uncertainty in the masses of the nonstrange $j^p = \frac{1}{2}^+$ charmed mesons, the $SU(3)$ splitting is far below theoretical expectations.

The $D_s(2317)$ and $D_s(2460)$ are only 40 MeV below the DK and D^*K threshold, respectively. This fact as well as the puzzles mentioned above have led to the hypothesis that they are bound states of $D^{(*)}$ and K [13–15]. Several papers analyze the spectroscopy of excited charm mesons by extending the quark model to include couplings to the DK continuum. This coupled channel effect has been analyzed within the quark model [16], chiral quark models [17,18] as well as unitarized meson models [19–21]. The unitarized meson model has also been used to make predictions for the spectroscopy of excited B mesons [20,22]. However, if one assumes that the $D_s(2317)$ and $D_s(2460)$ are nonrelativistic DK and D^*K bound states, respectively, heavy hadron chiral perturbation theory (HHχPT) [23] can be used to predict their electromagnetic branching ratios. These predictions are found to be in serious disagreement with experiment [24]. On the other hand, if one assumes that the $D_s(2317)$ and $D_s(2460)$ are conventional states, then HHχPT predictions for strong and electromagnetic decays are consistent with available data [24,25]. An alternative interpretation of these particles as exotic $c\bar{s}\,\bar{q}\,q$ tetraquarks has also been proposed [14,26–30]. For a review of theoretical work on $D_s(2317)$ and $D_s(2460)$, see Ref. [31].

In this paper we analyze the spectroscopy of charmed mesons using HHχPT. This theory can be used to analyze the low energy strong interactions of heavy mesons in a systematic expansion in light quark masses, m_q, and inverse heavy quark masses, $1/m_Q$. Nonanalytic corrections from loops with Goldstone bosons can be calculated in this formalism. The masses of the ground state heavy mesons have been studied in the heavy quark limit [32,33], including leading corrections from finite heavy quark masses and nonzero light quark masses [34–39]. These papers use a version of HHχPT which includes only the lowest lying $j^p = \frac{1}{2}^-$ heavy quark doublets. Many recent studies of excited $J^P = 0^+$ and 1^+ heavy mesons use Lagrangians that include only $j^p = \frac{1}{2}^-$ and $j^p = \frac{1}{2}^+$ heavy quark doublets as explicit degrees of freedom. However, the excited $j^p = \frac{3}{2}^+$ doublets are only separated from the $j^p = \frac{1}{2}^+$

doublets by $\lesssim 130$ MeV. Further, the $j^p = \frac{3}{2}^+$ doublets couple to the $j^p = \frac{1}{2}^+$ doublets at leading order in the chiral expansion, while the coupling of the $j^p = \frac{3}{2}^+$ doublets to the ground state doublets is higher order in the chiral expansion [40]. For these reasons, loops with virtual excited $j^p = \frac{3}{2}^+$ could have important effects on the physics of $j^p = \frac{1}{2}^+$ doublets. In this paper we will study the version of HHχPT containing only the $j^p = \frac{1}{2}^-$ and $j^p = \frac{1}{2}^+$ heavy quark doublets and leave investigation of loop effects from more highly excited states for future work.

A model of heavy mesons closely related to HHχPT is the parity doubling model of Refs. [41–44]. The parity doubling model is the analog of the linear sigma model for heavy mesons. Heavy meson doublets transforming linearly under $SU(3)_L \times SU(3)_R$ couple in a chirally invariant way to a field Σ transforming in the $(\bar{3}, 3)$ of $SU(3)_L \times SU(3)_R$. The field Σ develops a vacuum expectation value and the resulting theory of heavy mesons has the same form as HHχPT for the low lying odd- and even-parity doublets. Unlike HHχPT, the parity doubling model predicts relationships among otherwise independent parameters in the theory. One important prediction is that the hyperfine splittings of the $j^p = \frac{1}{2}^-$ and $j^p = \frac{1}{2}^+$ doublets are equal at tree level. This interesting prediction could partially explain the observed pattern of heavy meson hyperfine splittings, but it is not clear from Refs. [41–44] whether this prediction survives beyond tree level. This is a concern because loop corrections in HHχPT can be significant.

In this paper, we calculate the one-loop HHχPT corrections to the masses of $j^p = \frac{1}{2}^-$ and $j^p = \frac{1}{2}^+$ heavy meson doublets. We include all $O(1/m_Q)$ heavy quark spin-symmetry violating operators that appear to this order. A brief review of the HHχPT formalism is given in Sec. II and explicit formulas for the masses at one-loop appear in the Appendix. In Sec. III, we attempt to fit the observed mass spectrum with our one-loop formulas. The large number of free parameters makes it possible to reproduce the spectrum of $j^p = \frac{1}{2}^-$ and $j^p = \frac{1}{2}^+$ charmed mesons. In the $m_Q \to \infty$ limit our calculation of the difference of the $SU(3)$ splittings in HHχPT agrees with Ref. [45]. Our analysis differs from that in Ref. [45] in that we include $1/m_Q$ operators and perform a global fit to the spectrum with all counterterms treated as free parameters. In the approximation used in Ref. [45] there is a single counterterm constrained using lattice data.

In Sec. IV, we examine corrections to the hyperfine splittings and discuss the naturalness of the parity doubling model. The parity doubling model predicts that the hyperfine splittings and the magnitudes of the axial couplings of the $j^p = \frac{1}{2}^-$ and $j^p = \frac{1}{2}^+$ doublets are equal at tree level. We find that these parameter relations are preserved by the one-loop corrections so that the model provides a natural explanation for the equality of hyperfine splittings. Finally, in Sec. V, we use heavy quark effective theory (HQET) to estimate the masses of the $j^p = \frac{1}{2}^+$ B mesons, which have not yet been observed. These predictions may be helpful to experimentalists looking for these states.

II. HHχPT MASS COUNTERTERMS

In HHχPT, the ground state doublet is represented by the fields [23]

$$H_a = \frac{1 + \not{v}}{2}(H_a^\mu \gamma_\mu - H_a \gamma_5), \tag{3}$$

where a is an $SU(3)$ index. In the charm sector, H_a consists of the (D^0, D^+, D_s^+) pseudoscalar mesons and H_a^μ are the $(D^{*0}, D^{*+}, D_s^{*+})$ vector mesons. The $j^p = \frac{1}{2}^+$ doublet is represented by the fields [46]

$$S_a = \frac{1 + \not{v}}{2}(S_a^\mu \gamma_\mu \gamma_5 - S_a), \tag{4}$$

where the scalar states in the charm sector are $S_a = D_{0a}$ and the axial vectors are $S_a^\mu = D'_{1a}$. The kinetic terms of these fields are included in:

$$\begin{aligned}\mathcal{L}_v^{\text{kinetic}} = &-\text{Tr}[\overline{H}_a(iv \cdot D_{ba} - \delta_H \delta_{ab})H_b] \\ &+ \text{Tr}[\overline{S}_a(iv \cdot D_{ba} - \delta_S \delta_{ab})S_b],\end{aligned} \tag{5}$$

where δ_H and δ_S are the residual masses of the H and S fields, respectively, and D_{ba} is the chirally covariant derivative. In the theory with only H fields one is free to set $\delta_H = 0$. Since the only dimensionful parameters entering the loops in this theory are hyperfine splittings and meson masses, the UV divergences (in dimensional regularization) vanish in the $m_q \to 0$ and $m_Q \to \infty$ limit. Divergences in loop corrections are canceled by counterterms which are $O(m_q)$ or $O(1/m_Q)$. Once the S fields are added to the theory, there is another dimensionful quantity, $\delta_S - \delta_H$, which does not vanish as $m_q \to 0$ and $m_Q \to \infty$. The H self-energy diagrams with virtual S fields give a UV divergent contribution which survives in the $m_q \to 0$ and $m_Q \to \infty$ limit. Such a divergence must be canceled by a mass counterterm which respects $SU(3)$ and heavy quark spin symmetry and the only available counterterm is $\delta_H \text{Tr}\overline{H}_a H_a$. However, after one-loop divergences are canceled one is free to define the finite part of δ_H for convenience.

The fields have axial couplings to the pseudo-Goldstone bosons,

$$\begin{aligned}\mathcal{L}_v^{\text{axial}} = &\, g\,\text{Tr}[\overline{H}_a H_b \not{A}_{ba} \gamma_5] + g'\,\text{Tr}[\overline{S}_a S_b \not{A}_{ba} \gamma_5] \\ &+ h\,\text{Tr}[\overline{H}_a S_b \not{A}_{ba} \gamma_5 + \text{h.c.}],\end{aligned} \tag{6}$$

where g, g', and h are dimensionless constants to be determined from experiment. The other terms in the Lagrangian required are higher order mass counterterms. We use the notation of Ref. [38] and generalize it to include the S fields as well as the H fields.

$$\begin{aligned}\mathcal{L}_v^{\rm mass} = &-\frac{\Delta_H}{8}\,\mathrm{Tr}[\overline{H}_a\sigma^{\mu\nu}H_a\sigma_{\mu\nu}] + \frac{\Delta_S}{8}\,\mathrm{Tr}[\overline{S}_a\sigma^{\mu\nu}S_a\sigma_{\mu\nu}] + a_H\,\mathrm{Tr}[\overline{H}_aH_b]m^\xi_{ba} - a_S\,\mathrm{Tr}[\overline{S}_aS_b]m^\xi_{ba} + \sigma_H\,\mathrm{Tr}[\overline{H}_aH_a]m^\xi_{bb}\\ &- \sigma_S\,\mathrm{Tr}[\overline{S}_aS_a]m^\xi_{bb} - \frac{\Delta_H^{(a)}}{8}\,\mathrm{Tr}[\overline{H}_a\sigma^{\mu\nu}H_b\sigma_{\mu\nu}]m^\xi_{ba} + \frac{\Delta_S^{(a)}}{8}\,\mathrm{Tr}[\overline{S}_a\sigma^{\mu\nu}S_b\sigma_{\mu\nu}]m^\xi_{ba} - \frac{\Delta_H^{(\sigma)}}{8}\,\mathrm{Tr}[\overline{H}_a\sigma^{\mu\nu}H_a\sigma_{\mu\nu}]m^\xi_{bb}\\ &+ \frac{\Delta_S^{(\sigma)}}{8}\,\mathrm{Tr}[\overline{S}_a\sigma^{\mu\nu}S_a\sigma_{\mu\nu}]m^\xi_{bb}, \end{aligned} \tag{7}$$

where $m^\xi_{ba} = \frac{1}{2}(\xi m_q\xi + \xi^\dagger m_q\xi^\dagger)_{ba}$, $m_q = \mathrm{diag}(m_u, m_d, m_s)$ and $\xi = \sqrt{\Sigma} = \exp(i\Pi/f)$, where Π is the matrix of Goldstone bosons. The Δ_H and Δ_S terms in Eq. (7) are spin-symmetry violating operators which give rise to hyperfine splittings. The a_H, a_S, σ_H, and σ_S terms are $O(m_q)$ and preserve heavy quark spin symmetry. The remaining terms are $O(m_q)$ and violate heavy quark spin symmetry.

At tree level the residual masses are

$$\begin{aligned} m^0_{H_a} &= \delta_H - \frac{3}{4}\Delta_H + \sigma_H\overline{m} + a_Hm_a - \frac{3}{4}\Delta_H^{(\sigma)}\overline{m} - \frac{3}{4}\Delta_H^{(a)}m_a\\ m^0_{H_a^*} &= \delta_H + \frac{1}{4}\Delta_H + \sigma_H\overline{m} + a_Hm_a + \frac{1}{4}\Delta_H^{(\sigma)}\overline{m} + \frac{1}{4}\Delta_H^{(a)}m_a\\ m^0_{S_a} &= \delta_S - \frac{3}{4}\Delta_S + \sigma_S\overline{m} + a_Sm_a - \frac{3}{4}\Delta_S^{(\sigma)}\overline{m} - \frac{3}{4}\Delta_S^{(a)}m_a\\ m^0_{S_a^*} &= \delta_S + \frac{1}{4}\Delta_S + \sigma_S\overline{m} + a_Sm_a + \frac{1}{4}\Delta_S^{(\sigma)}\overline{m} + \frac{1}{4}\Delta_S^{(a)}m_a, \end{aligned} \tag{8}$$

where $m_a = (m_u, m_d, m_s)$ and $\overline{m} = m_u + m_d + m_s$. Here the asterisk denotes the spin-1 member of the heavy quark doublet. In the isospin limit $m_u = m_d$. HHχPT is a double expansion in $\Lambda_{\rm QCD}/m_Q$ and Q/Λ_χ, where $Q \sim m_\pi$, m_K, m_η and $\Lambda_\chi = 4\pi f \approx 1.5$ GeV. The parameters δ_H, δ_S, Δ_H, and Δ_S are treated as $O(Q)$ in the power counting [24]. Since $m_q \propto m_\pi^2 \sim Q^2$ the remaining terms in Eq. (8) are formally higher order in the power counting. The loop corrections to the masses are shown in Fig. 1. Single lines represent the H fields and double lines represent the S fields. All diagrams are $O(Q^3)$. The loop corrections are regulated using dimensional regularization. Complete one-loop expressions for the masses are given in the Appendix.

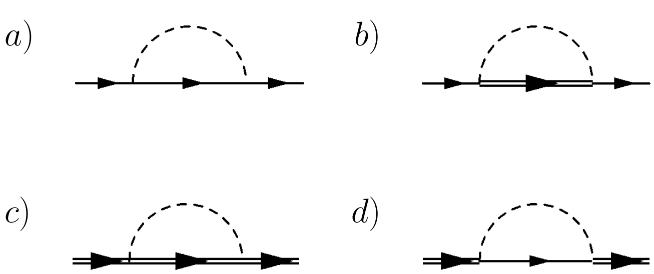

FIG. 1. One-loop self-energy diagrams for the H and S fields. H fields are single lines, S fields are double lines and Goldstone bosons are dashed lines.

III. CHARMED MESON SPECTRUM

In this section we analyze the charmed meson spectrum using the one-loop mass formulas given in the Appendix. We will work in the isospin limit, where the masses of H_1 and H_2, for instance, are identical. Then there are eight different residual masses: m_{H_1}, m_{H_3}, $m_{H_1^*}$, $m_{H_3^*}$, m_{S_1}, m_{S_3}, $m_{S_1^*}$, and $m_{S_3^*}$. To determine the experimental values of m_{H_1} and $m_{H_1^*}$, we average the masses of the two known isospin states. The residual masses are defined to be the difference between the real masses and an arbitrarily chosen reference mass of $O(m_Q)$. We will measure all masses relative to the nonstrange spin averaged H mass, so $(m_{H_1} + 3m_{H_1^*})/4 = 0$. Therefore, the experimentally measured residual masses we will fit to are:

$$\begin{aligned} m_{H_1} &= -106.1\ \mathrm{MeV} & m_{H_3} &= -4.75\ \mathrm{MeV}\\ m_{H_1^*} &= 35.4\ \mathrm{MeV} & m_{H_3^*} &= 139.1\ \mathrm{MeV}\\ m_{S_1} &= 335.0\ \mathrm{MeV} & m_{S_3} &= 344.4\ \mathrm{MeV}\\ m_{S_1^*} &= 465.0\ \mathrm{MeV} & m_{S_3^*} &= 486.3\ \mathrm{MeV}. \end{aligned} \tag{9}$$

The tree-level expressions in Eq. (8) reproduce these values with $\delta_S + \sigma_S\overline{m} - \delta_H - \sigma_H\overline{m} = 432 \pm 26$ MeV, $\Delta_H + \Delta_H^{(\sigma)}\overline{m} = 146 \pm 1$ MeV, $\Delta_S + \Delta_S^{(\sigma)}\overline{m} = 129 \pm 50$ MeV, $a_H = 1.14 \pm 0.06$, $a_S = 0.21 \pm 0.29$, $\Delta_H^{(a)} = -0.03 \pm 0.01$, and $\Delta_S^{(a)} = 0.14 \pm 0.55$. The errors used to obtain this fit are the experimental ones, dominated by the uncertainty in the nonstrange 0^+ and 1^+ masses. This gives rise to the large uncertainties seen in parameters in the Lagrangian involving the S fields. The fits presented in this section use Mathematica [47] and/or Minuit [48].

The loop corrections depend on 11 parameters: g, g', h, a_H, a_S, $\Delta_H^{(a)}$, $\Delta_S^{(a)}$, $\delta_H + \sigma_H\overline{m}$, $\delta_S + \sigma_S\overline{m}$, $\Delta_H + \Delta_H^{(\sigma)}\overline{m}$, and $\Delta_S + \Delta_S^{(\sigma)}\overline{m}$. The parameters σ_H, σ_S, $\Delta_H^{(\sigma)}$, and $\Delta_S^{(\sigma)}$ cannot be separately determined because they always appear in linear combination with the parameters δ_H, δ_S, Δ_H, and Δ_S, respectively. Below we will absorb the contribution of the parameters σ_H, σ_S, $\Delta_H^{(\sigma)}$, and $\Delta_S^{(\sigma)}$ into the measured values of δ_H, δ_S, Δ_H, and Δ_S, respectively.

An analysis of D^* decays using a one-loop calculation without explicit excited states yields $g = 0.27^{+0.06}_{-0.03}$ [49]. From the widths of the nonstrange resonances observed by Belle we have extracted $h = 0.69 \pm 0.09$ at tree level [24]. Both couplings are of order unity and therefore consistent with naive power counting. The remaining parameters are unknown.

We use $f = 120$ MeV, which is the value extracted in Ref. [49] using the one-loop formulas for pion and kaon decay constants, first derived in Ref. [50]. We set $m_u = m_d = 4$ MeV and $m_s = 90$ MeV. Below we show several different fits. In the first case we fix g and h to the values (given above) extracted from previous analyses. This leaves nine remaining free parameters. Performing a least chi-squared fit to the meson spectrum, using experimental uncertainties, we obtain the following central values

$$\begin{aligned} m_{H_1} &= -106 \text{ MeV} & m_{H_3} &= -5 \text{ MeV} \\ m_{H_1^*} &= 35 \text{ MeV} & m_{H_3^*} &= 139 \text{ MeV} \\ m_{S_1} &= 160 \text{ MeV} & m_{S_3} &= 344 \text{ MeV} \\ m_{S_1^*} &= 296 \text{ MeV} & m_{S_3^*} &= 486 \text{ MeV}. \end{aligned} \tag{10}$$

The parameters extracted from this fit are: $g' = 0.09 \pm 0.03$, $\delta_H = -83 \pm 3$ MeV, $\delta_S = 244 \pm 1$ MeV, $\Delta_H = 133 \pm 2$ MeV, $\Delta_S = 136 \pm 1$ MeV, $a_H = 1.70 \pm 0.01$, $a_S = 0.25 \pm 0.08$, $\Delta_H^{(a)} = -0.07 \pm 0.01$, and $\Delta_S^{(a)} = 0.04 \pm 0.03$. Six of the mass parameters are reproduced quite well while m_{S_1} and $m_{S_1^*}$ are lower than the central values of experiments by about 175 and 169 MeV, respectively. This qualitative picture persists without much sensitivity to the value of g'. However, these fits are not very good and such a procedure may not be very realistic. The values of g and h used above were extracted using a fit to a one-loop calculation not including the S fields, and a tree-level fit, respectively. There is no reason to believe that these values are the ones which are appropriate for a calculation that includes graphs with internal S states. Note that large changes between tree- versus loop-extracted parameter values do not necessarily indicate poor convergence; what is important is that the observables do not suffer large changes between orders.

If we include g and h as free parameters in an 11-parameter fit, there are many solutions which yield central values identical to the experimental residual masses given in Eq. (9). In addition to the experimental errors we also include 20% "theoretical" errors to mimic the fact that our analysis is only accurate to $\mathcal{O}(Q^3)$. The masses obtained are then accompanied by errors at the $\pm$ 30 to 40 MeV level. Examples of parameter sets which give these results are:

(a) $|g| = 1.15 \pm 0.06$, $|g'| = 0.90 \pm 0.06$, $|h| = 2.3 \pm 0.2$, $\delta_H = 195 \pm 41$ MeV, $\delta_S = 332 \pm 31$ MeV, $\Delta_H = 465 \pm 24$ MeV, $\Delta_S = 597 \pm 28$ MeV, $a_H = 7 \pm 1$, $a_S = -4 \pm 1$, $\Delta_H^{(a)} = -4.4 \pm 0.7$, and $\Delta_S^{(a)} = -10 \pm 2$.

(b) $|g| = 0.65 \pm 0.06$, $|g'| = 0.89 \pm 0.08$, $|h| = 0.2 \pm 0.1$, $\delta_H = 117 \pm 21$ MeV, $\delta_S = 646 \pm 40$ MeV, $\Delta_H = 68 \pm 42$ MeV, $\Delta_S = 447 \pm 23$ MeV, $a_H = 3.8 \pm 0.7$, $a_S = 3.1 \pm 0.7$, $\Delta_H^{(a)} = -0.3 \pm 1$, and $\Delta_S^{(a)} = -2.8 \pm 1$.

(c) $|g| = 0.89 \pm 0.07$, $|g'| = 0.24 \pm 0.13$, $|h| = 0.98 \pm 0.11$, $\delta_H = 203 \pm 39$ MeV, $\delta_S = 399 \pm 26$ MeV, $\Delta_H = 242 \pm 25$ MeV, $\Delta_S = 116 \pm 59$ MeV, $a_H = 5.8 \pm 1.1$, $a_S = -1.4 \pm 1.5$, $\Delta_H^{(a)} = -1.7 \pm 0.8$, and $\Delta_S^{(a)} = 2.1 \pm 1.7$.

(d) $|g| = |g'| = 0.70 \pm 0.03$, $|h| = 2.4 \pm 0.2$, $\delta_H = 114 \pm 64$ MeV, $\delta_S = 231 \pm 36$ MeV, $\Delta_H = 682 \pm 4$ MeV, $a_H = 4.3 \pm 0.7$, $a_S = -3.0 \pm 2.1$, $\Delta_H^{(a)} = -0.89 \pm 0.96$, and $\Delta_S^{(a)} = -2.7 \pm 0.9$. (In this fit, the constraint $\Delta_S = \Delta_H + 30$ MeV was used.)

There are clearly many local minima which Minuit [48] may find. Some of these values of g and h significantly exceed values extracted from experiment in Refs. [49,51] and Ref. [24], respectively. They also exceed estimates based on the quark model [52], extraction from lattice QCD simulations [53,54] as well as sum rule constraints [55]. Again, however, it is not clear what can be concluded when comparing parameters which are by themselves unphysical and whose definition depends upon the details of a calculation. Of perhaps more concern is that these fits produce large values for the hyperfine coefficients. The operators which cause hyperfine splitting should be $1/m_Q$ suppressed compared to the leading order ones. Set (d) is an example of a solution where $|g|$ is near $|g'|$ and Δ_S is within 30 MeV of Δ_H. The relevance of that result will become apparent in the next section. Finally, an example fit where g and h are restricted to lie between 0 and 1 yields central values of parameters as follows:

$$\begin{gathered} |g| = 0.43, \qquad |g'| = 0, \qquad h = 0.31, \\ \delta_H = 25 \text{ MeV}, \qquad \delta_S = 443 \text{ MeV}, \\ \Delta_H = 124 \text{ MeV}, \qquad \Delta_S = 131 \text{ MeV}, \qquad a_H = 2.4, \\ a_S = -0.3, \qquad \Delta_H^{(a)} = -0.2, \qquad \Delta_S^{(a)} = 0.1. \end{gathered}$$

These parameter values lead to a prediction for the mass spectrum that also agrees with Eq. (9).

The underconstrained nature of the various fits makes strong conclusions impossible. In particular, the uncertainty in the parameter space is very large and the uncertainty in individual parameters is much greater than indicated by the errors quoted in the individual fits listed above. The situation should improve with a global fit to both masses and decay rates which uses a consistent set of next-to-leading order calculations that include the excited states. This work is in progress.

IV. HYPERFINE SPLITTINGS

In this section we study the one-loop corrections to the hyperfine splittings to see if HHχPT can provide insight into the observed near equality of the hyperfine splittings. Using the formulas in the Appendix we find that the next-to-leading order difference between even-parity and odd-parity hyperfine splittings in the strange sector is given by

$$\begin{aligned}(m_{S_3^*} - m_{S_3}) - (m_{H_3^*} - m_{H_3}) = {} & (m^0_{S_3^*} - m^0_{S_3}) - (m^0_{H_3^*} - m^0_{H_3}) + \frac{g'^2}{f^2}\bigg[\frac{2}{3}K_1(m^0_{S_1} - m^0_{S_3^*}, m_K) + \frac{2}{9}K_1(m^0_{S_3} - m^0_{S_3^*}, m_\eta) \\ & + \frac{4}{3}K_1(m^0_{S_1^*} - m^0_{S_3^*}, m_K) + \frac{4}{9}K_1(0, m_\eta) - 2K_1(m^0_{S_1^*} - m^0_{S_3}, m_K) - \frac{2}{3}K_1(m^0_{S_3^*} - m^0_{S_3}, m_\eta)\bigg] \\ & - \frac{g^2}{f^2}\bigg[\frac{2}{3}K_1(m^0_{H_1} - m^0_{H_3^*}, m_K) + \frac{2}{9}K_1(m^0_{H_3} - m^0_{H_3^*}, m_\eta) + \frac{4}{3}K_1(m^0_{H_1^*} - m^0_{H_3^*}, m_K) \\ & + \frac{4}{9}K_1(0, m_\eta) - 2K_1(m^0_{H_1^*} - m^0_{H_3}, m_K) - \frac{2}{3}K_1(m^0_{H_3^*} - m^0_{H_3}, m_\eta)\bigg] \\ & + \frac{h^2}{f^2}\bigg[2K_2(m^0_{H_1^*} - m^0_{S_3^*}, m_K) + \frac{2}{3}K_2(m^0_{H_3^*} - m^0_{S_3^*}, m_\eta) - 2K_2(m^0_{H_1} - m^0_{S_3}, m_K) \\ & - \frac{2}{3}K_2(m^0_{H_3} - m^0_{S_3}, m_\eta) - 2K_2(m^0_{S_1^*} - m^0_{H_3^*}, m_K) - \frac{2}{3}K_2(m^0_{S_3^*} - m^0_{H_3^*}, m_\eta) \\ & + 2K_2(m^0_{S_1} - m^0_{H_3}, m_K) + \frac{2}{3}K_2(m^0_{S_3} - m^0_{H_3}, m_\eta)\bigg]. \end{aligned} \tag{11}$$

Suppose one imposes at tree level the condition that all hyperfine splittings in each of the doublets are degenerate:

$$m^0_{H_a^*} - m^0_{H_a} = m^0_{S_a^*} - m^0_{S_a} = \Delta. \tag{12}$$

This can be arranged by invoking the tree-level prediction of the parity doubling model, $\Delta_H = \Delta_S = \Delta$ and neglecting the terms proportional to m_q in Eq. (8), which are formally higher order in the power counting. Then $m^0_{S_a^*} - m^0_{H_a^*} = m^0_{S_a} - m^0_{H_a}$ and it is easy to verify that all contributions proportional to h^2 vanish, and the remaining terms are:

$$\begin{aligned}(m_{S_3^*} - m_{S_3}) - (m_{H_3^*} - m_{H_3}) = {} & \frac{g'^2}{f^2}\bigg[\frac{2}{3}K_1(-\Delta, m_\pi) + \frac{2}{9}K_1(-\Delta, m_\eta) + \frac{16}{9}K_1(0, m_K) - 2K_1(\Delta, m_K) - \frac{2}{3}K_1(\Delta, m_\eta)\bigg] \\ & - \frac{g^2}{f^2}\bigg[\frac{2}{3}K_1(-\Delta, m_\pi) + \frac{2}{9}K_1(-\Delta, m_\eta) + \frac{16}{9}K_1(0, m_K) - 2K_1(\Delta, m_K) - \frac{2}{3}K_1(\Delta, m_\eta)\bigg]. \end{aligned} \tag{13}$$

This vanishes if $g^2 = g'^2$, which is consistent with the parity doubling model prediction. A similar cancellation occurs for the nonstrange hyperfine splittings. So the parity doubling model explanation for the equality of the $j^p = \frac{1}{2}^-$ and $\frac{1}{2}^+$ hyperfine splittings is robust in the sense that one-loop corrections do not spoil the prediction.

The parity doubling model prediction for the axial couplings and hyperfine splittings singles out a subspace of the parameter space of HHχPT that is preserved under renormalization group evolution. From our mass formulas it is easy to derive the following renormalization group equations for the renormalized parameters Δ_H and Δ_S:

$$\mu^2\frac{d}{d\mu^2}\Delta_H = \frac{4g^2}{9\pi^2 f^2}\Delta_H^3 - \frac{h^2}{3\pi^2 f^2}(\Delta_S - \Delta_H)\bigg[3(\delta_S - \delta_H)^2 - \frac{3}{2}(\Delta_S - \Delta_H)(\delta_S - \delta_H) + \frac{7}{16}(\Delta_S - \Delta_H)^2\bigg], \tag{14}$$

$$\mu^2\frac{d}{d\mu^2}\Delta_S = \frac{4g'^2}{9\pi^2 f^2}\Delta_S^3 + \frac{h^2}{3\pi^2 f^2}(\Delta_S - \Delta_H)\bigg[3(\delta_S - \delta_H)^2 - \frac{3}{2}(\Delta_S - \Delta_H)(\delta_S - \delta_H) + \frac{7}{16}(\Delta_S - \Delta_H)^2\bigg]. \tag{15}$$

This leads to

$$\begin{aligned}\mu^2\frac{d}{d\mu^2}(\Delta_S - \Delta_H) = {} & \frac{4}{9\pi^2 f^2}(g'^2\Delta_S^3 - g^2\Delta_H^3) + \frac{2h^2}{3\pi^2 f^2}(\Delta_S - \Delta_H)\bigg[3(\delta_S - \delta_H)^2 - \frac{3}{2}(\Delta_S - \Delta_H)(\delta_S - \delta_H) \\ & + \frac{7}{16}(\Delta_S - \Delta_H)^2\bigg]. \end{aligned} \tag{16}$$

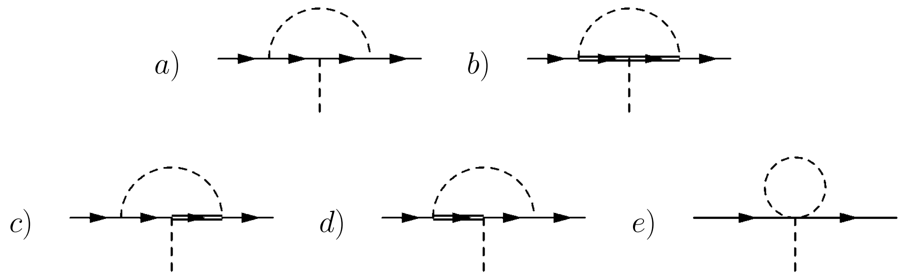

FIG. 2. One-loop diagrams for renormalization of the coupling g. H fields are single lines, S fields are double lines and Goldstone bosons are dotted lines. Diagrams for renormalization of the coupling g' are obtained by interchanging H and S fields.

We also derive the one-loop renormalization group equation for the couplings g and g'. For this we need the wavefunction renormalization of the fields H and S, which is obtained from the graphs in Fig. 1, and the one-loop corrections to the axial couplings. The relevant graphs for the renormalization of g are shown in Fig. 2, and the graphs for g' can be obtained from those in Fig. 2 by interchanging H and S lines. Note that we only need the ultraviolet divergences of these graphs to obtain the renormalization group equation. Furthermore, the counterterms for the wavefunction renormalization and the axial couplings are defined to be independent of m_q and m_Q.[2] Ultraviolet divergences proportional to m_q and $1/m_Q$ are absorbed into higher order counterterms. For example, a divergence proportional to m_q in the one-loop correction to the axial coupling of the H fields should be renormalized by counterterms with structures like $\mathrm{Tr}[\overline{H}_a H_b \not{A}_{bc}\gamma_5]m^{\xi}_{ca}$, $\mathrm{Tr}[\overline{H}_a H_b \not{A}_{ba}\gamma_5]m^{\xi}_{cc}$, etc. Therefore we can ignore Goldstone boson masses and hyperfine splittings in computing the ultraviolet divergences, which greatly simplifies the calculation. The graphs in Figs. 1(a), 1(c), 2(a), and 2(e) vanish in this limit because the integrals are scaleless. Graphs in Figs. 2(c) and 2(d) do not contribute either. This is because the H-S-π coupling in Figs. 2(c) and 2(d) gives a factor of $v \cdot k$, where k^μ is the four-momentum of the external Goldstone boson. Ultraviolet divergences in Figs. 2(c) and 2(d) are proportional to $v \cdot k$ and are canceled by counterterms with an additional covariant derivative acting on the fields A^μ_{ab}, such as $\mathrm{Tr}[\overline{H}_a H_b i v \cdot D_{bc} \not{A}_{ca}\gamma_5]$. Therefore, all that is needed to obtain the running of g are the ultraviolet divergent parts of Figs. 1(b) and 2(b) in the limit where Goldstone bosons and hyperfine splittings are neglected. The running of g' is obtained from Fig. 1(d) and the analog of Fig. 2(b) with S and H lines interchanged. The result can be obtained from the corresponding graphs for the renormalization of g by simply substituting $g \leftrightarrow g'$ and $\delta_S - \delta_H \to -(\delta_S - \delta_H)$. The renormalization group equations for g and g' are

$$\mu \frac{d}{d\mu} g = -\frac{h^2}{4\pi^2 f^2}(\delta_S - \delta_H)^2(g' + 8g)$$
$$\mu \frac{d}{d\mu} g' = -\frac{h^2}{4\pi^2 f^2}(\delta_H - \delta_S)^2(g + 8g'), \tag{17}$$

which can be rewritten as

$$\mu \frac{d}{d\mu}(g + g') = -\frac{9h^2}{4\pi^2 f^2}(\delta_H - \delta_S)^2(g + g')$$
$$\mu \frac{d}{d\mu}(g - g') = -\frac{7h^2}{4\pi^2 f^2}(\delta_H - \delta_S)^2(g - g'). \tag{18}$$

To understand the significance of this result, consider the naive quark model prediction $g' = g/3$ [40]. From the renormalization group equations in Eq. (17) one sees that g and g' vary with changes of the renormalization scale in such a way that the condition $g' = g/3$ can only hold at one value of μ. The quark model prediction is meaningless beyond tree level without also specifying a particular renormalization scheme and scale at which the relation is expected to hold. However, if $g = \pm g'$ holds at any μ, it will hold for all μ (at least at one-loop order). Also, if $g^2 = g'^2$ and $\Delta_S = \Delta_H$ the right hand side of Eq. (16) vanishes. Thus the predictions of the parity doubling model, $\Delta_H = \Delta_S$ and $g = -g'$, are invariant under renormalization group flow in HHχPT to one-loop order.

V. HQET AND PREDICTIONS FOR EXCITED B MESONS

In this section, we comment on the theoretical expectations for the spectrum of excited even-parity bottom mesons which have yet to be discovered. Our HHχPT results for the charmed meson spectrum may be used, but there are unknown $O(1/m_Q)$ effects which make it difficult to obtain precise predictions for the B mesons. For finite quark masses, to obtain the bottom meson spectrum from the charmed meson results, the hyperfine operators should be rescaled by m_c/m_b, which is not very well determined. Other parameters can receive $O(\Lambda_{\mathrm{QCD}}/m_c - \Lambda_{\mathrm{QCD}}/m_b)$ corrections. For instance, the reduced kinetic energy of the b quark significantly reduces the mass splitting of the

[2]If the theory is not renormalized this way, dependence on the underlying theory parameters m_q and m_Q would no longer be explicit in the chiral Lagrangian.

H and S doublets in the b sector relative to what is observed in the charmed system. These $O(1/m_Q)$ corrections introduce significant uncertainty in HHχPT predictions.

We will instead use the $O(1/m_Q)$ HQET formulas for the mass of a heavy hadron X which contains a heavy quark Q [56]:

$$m_X^{(Q)} = m_Q + \bar{\Lambda}^X - \frac{\lambda_1^X}{2m_Q} + n_J \frac{\lambda_2^X}{2m_Q}, \tag{19}$$

where λ_1^X and λ_2^X are hadronic matrix elements of the HQET operators $\bar{h}(iD)^2 h$ and $g_s \bar{h}\sigma^{\mu\nu}G_{\mu\nu}h/2$, respectively, and $n_J = +1$ for $J = 1$ states and $n_J = -3$ for $J = 0$ states. The first $1/m_Q$ correction, $-\lambda_1^X/(2m_Q)$, is the kinetic energy of the heavy quark. The second $1/m_Q$ correction contributes to hyperfine splittings. The difference between the spin averaged masses of the $j^P = \frac{1}{2}^-$ and $j^P = \frac{1}{2}^+$ mesons, $\overline{m}_H^{(Q)} = (3m_{H^*}^{(Q)} + m_H^{(Q)})/4$ and $\overline{m}_S^{(Q)} = (3m_{S^*}^{(Q)} + m_S^{(Q)})/4$, respectively, is given by

$$\overline{m}_S^{(Q)} - \overline{m}_H^{(Q)} = \bar{\Lambda}^S - \bar{\Lambda}^H - \frac{\lambda_1^S}{2m_Q} + \frac{\lambda_1^H}{2m_Q}, \tag{20}$$

which leads to the following formulas for the splitting of the even- and odd-parity states in the bottom sector:

$$\overline{m}_S^{(b)} - \overline{m}_H^{(b)} = \overline{m}_S^{(c)} - \overline{m}_H^{(c)} + (\lambda_1^S - \lambda_1^H)\left(\frac{1}{2m_c} - \frac{1}{2m_b}\right). \tag{21}$$

A recent global fit to B decays yields $\lambda_1^H = -0.20 \pm 0.06\ \mathrm{GeV}^2$ [57]. The parameter λ_1^S is unknown. From the spectroscopy of excited $j^P = \frac{3}{2}^+$ D and B mesons, Ref. [58] extracts $\lambda_1^{3/2} - \lambda_1^H = -0.23\ \mathrm{GeV}^2$, where $\lambda_1^{3/2}$ is the λ_1 matrix element for the $j^P = \frac{3}{2}^+$ doublet. The sign here indicates that the kinetic energy of the heavy quark in the excited heavy meson is larger than that in the ground state, which agrees with intuition. We expect the kinetic energy of the heavy quark in the $j^P = \frac{1}{2}^+$ states to be comparable to that of $j^P = \frac{3}{2}^+$ states. To estimate $\overline{m}_S^{(b)}$ with conservative errors, we take $\lambda_1^S - \lambda_1^H = -0.2 \pm 0.1\ \mathrm{GeV}^2$, $m_c = 1.4$ GeV, and $m_b = 4.8$ GeV to find

$$\overline{m}_S^{(b)} - \overline{m}_H^{(b)} = \overline{m}_S^{(c)} - \overline{m}_H^{(c)} - 50 \pm 25\ \mathrm{MeV}. \tag{22}$$

In the bottom nonstrange sector, $m_{H_1}^{(b)} = 5279$ MeV and $m_{H_1^*}^{(b)} = 5325$ MeV, which yields $\overline{m}_{H_1}^{(b)} = 5314$ MeV and therefore Eq. (22) predicts $\overline{m}_{S_1}^{(b)} = 5696 \pm 30 \pm 25$ MeV. The first error comes from the uncertainty in the charm nonstrange $j^P = \frac{1}{2}^+$ masses and the second is the estimated uncertainty in λ_1^S. These states are well above the threshold for S-wave pion decays to the ground state and should be broad like their charm counterparts.

In the bottom strange sector, only the 0^- state with mass $m_{H_3}^{(b)} = 5370$ MeV has been observed. To proceed we need to estimate the mass of the bottom strange 1^- state. Note that

$$\frac{m_{H^*}^{(b)} - m_H^{(b)}}{m_{H^*}^{(c)} - m_H^{(c)}} = \frac{m_{S^*}^{(b)} - m_S^{(b)}}{m_{S^*}^{(c)} - m_S^{(c)}} = \frac{m_c}{m_b}. \tag{23}$$

up to $O(1/m_Q)$ corrections. Thus, all the hyperfine splittings in the bottom sector are related to those in the charm sector by a universal factor. Combining this with the measured value of $m_{H_1^*}^{(b)} - m_{H_1}^{(b)}$ leads to the prediction that $m_{H_3^*}^{(b)} - m_{H_3}^{(b)} = m_{S_3^*}^{(b)} - m_{S_3}^{(b)} = 46$ MeV, and $m_{S_1^*}^{(b)} - m_{S_1}^{(b)} = 42$ MeV. These predictions have approximately 25% uncertainty due to higher order $O(\Lambda_{\mathrm{QCD}}/m_c - \Lambda_{\mathrm{QCD}}/m_b)$ corrections and the prediction for $m_{S_1^*}^{(b)} - m_{S_1}^{(b)}$ estimate has an additional 20% uncertainty due to the poorly known $m_{S_1^*}^{(c)}$ and $m_{S_1}^{(c)}$ masses. Given these hyperfine splittings, one expects $\overline{m}_{H_3}^{(b)} = 5404$ MeV and then Eq. (22) predicts $\overline{m}_{S_3}^{(b)} = 5702 \pm 25$ MeV. Here the error is dominated by our ignorance of λ_S^1. Note that the excited bottom strange mesons are expected to lie well below the threshold for decays to ground state B mesons and kaons and should be narrow like $j^P = \frac{1}{2}^+$ charmed strange mesons.

VI. CONCLUSIONS

We have enumerated the leading and subleading operators which describe the even-parity charmed meson masses in heavy hadron chiral perturbation theory (HHχPT). We performed a loop calculation to analyze the lowest lying even- and odd-parity charmed meson masses to $\mathcal{O}(Q^3)$. There are nominally 11 unknown parameters in the prediction, and only eight experimental masses. Two of the parameters, the axial coupling g for the lowest doublet of charmed mesons, and the coupling h which dominates the strong decay between the even-parity and ground state doublets, have been extracted from previous calculations. See Ref. [49] and Ref. [24], respectively. However, the even-parity states were not included in the extraction of g in Ref. [49]. Also, the extraction of h was only performed at tree level. Since these values for g and h were not obtained under the same conditions as the mass calculations performed in this paper, it is not clear that the values should be used in our fit. Indeed, if the values from Refs. [24,49] are used, it is not possible to obtain the nonstrange even-parity masses as large as they are observed to be. If the g and h parameters are not fixed but simply constrained to lie between 0 and 1, which is the prejudice from other analyses, then a fit to the even-parity masses is possible. Because of the numerous undetermined parameters, HHχPT can accommodate, but not explain, the unusual pattern of $SU(3)$ breaking observed in the excited charmed meson spectrum.

If we perform an unconstrained fit to the charmed meson mass spectrum using all 11 parameters, many solutions are possible, including ones whose values of g and h are not unreasonably far from their previously extracted values. However, then the parameter values found for the hyperfine operators are of concern. These hyperfine operators should have coefficients which scale as $\mathcal{O}(\Lambda_{\rm QCD}^2/m_Q)$ relative to the $\mathcal{O}(\Lambda_{\rm QCD})$ coefficients of the leading operators. The fact that unconstrained global fits find coefficients which are sometimes larger for the hyperfine operators than for the leading order operators may signal a problem in the $1/m_Q$ expansion. On the other hand, this may simply be a consequence of not properly incorporating the constraints on g and h from the decay widths. Before more definitive statements can be made, a global fit including even-parity intermediate states and terms up to $\mathcal{O}(Q^3)$ for both the odd-parity and even-parity meson decay rates must be done. That will be the subject of a subsequent paper.

Next we consider the parity doubling model introduced in Refs. [41–44]. While the parity doubling model is not a result of QCD, but requires additional assumptions, it is interesting because it provides an explanation of the observed equality of the hyperfine splitting in the even-parity doublet and the hyperfine splitting in the odd-parity doublet. QCD symmetries alone do not dictate any relationship between these hyperfine splittings. While the parity doubling model provides an explanation for the equality of the hyperfine splittings, the question we address here is whether it is a *natural* explanation. That is, does it survive beyond tree level? Is it stable under renormalization group flow? We find that there are "fixed lines" at $|g| = |g'|$. (These are axial operator coefficients from Eq. (6).) That is, if at any time in their evolution $g = g'$ or $g = -g'$, renormalization group analysis shows that the relationship will be maintained. This in turn assures that if at tree level the parameters Δ_H and Δ_S in Eq. (7) are equal, they remain so to one-loop. This lends credence to the parity doubling model. The stability found in the parity doubling model does not exist for other models, such as the nonrelativistic quark model, which predicts $g' = g/3$. Going back to the parameter fit, we do find that solutions with $|g|$ near $|g'|$ are possible, as are fits with Δ_H near Δ_S. However, such fits yield values for Δ_H and Δ_S which are larger than expected by power counting. In addition, there are fits which reproduce the observed hyperfine splittings without $|g| \approx |g'|$.

Finally, we discuss how the charmed meson spectrum results can be used to make predictions for the analog B meson spectrum. It is necessary to know the charm and bottom quark masses in order to rescale the operators, which brings in significant uncertainty. Also, there are additional $1/m_Q$ operators with unknown parameters. However, it is possible to use heavy quark effective theory to estimate that the even-parity strange spin-zero B meson has mass $\sim$5667 MeV while its spin-one partner has mass $\sim$5714 MeV. This places them below the threshold for decay to a kaon and the ground state B. Therefore, we expect narrow B_s^* meson analogs to the narrow D_s^* excited mesons.

ACKNOWLEDGMENTS

R. P. S. and T. M. are supported in part by DOE Grant No. DE-FG02-96ER40945. T. M. is also supported in part by DOE Grant No. DE-AC05-84ER40150. T. M. would like to thank the Aspen Center for Physics and the KITP in Santa Barbara where parts of this work were completed.

APPENDIX

We express our results in terms of the functions

$$\begin{aligned} K_1(\eta, M) &= \frac{1}{16\pi^2}\bigg[(-2\eta^3 + 3M^2\eta)\ln\bigg(\frac{M^2}{\mu^2}\bigg) \\ &\quad + 2\eta(\eta^2 - M^2)F\bigg(\frac{\eta}{M}\bigg) + 4\eta^3 - 5\eta M^2\bigg] \\ K_2(\eta, M) &= \frac{1}{16\pi^2}\bigg[(-2\eta^3 + M^2\eta)\ln\bigg(\frac{M^2}{\mu^2}\bigg) \\ &\quad + 2\eta^3 F\bigg(\frac{\eta}{M}\bigg) + 4\eta^3 - \eta M^2\bigg], \end{aligned} \tag{A1}$$

where

$$F(x) = 2\frac{\sqrt{1-x^2}}{x}\bigg[\frac{\pi}{2} - \tan^{-1}\bigg(\frac{x}{\sqrt{1-x^2}}\bigg)\bigg] \quad |x| < 1 \tag{A2}$$

$$= -2\frac{\sqrt{x^2-1}}{x}\ln(x + \sqrt{x^2-1}) \quad |x| > 1 \tag{A3}$$

The function $K_1(\eta, M)$ appears whenever the virtual heavy meson inside the loop is in the same doublet as the external heavy meson, while $K_2(\eta, M)$ appears when the virtual heavy meson is from the opposite parity doublet.

In the limit $M \ll \eta$ these functions become

$$\begin{aligned} K_1(\eta, M) &= \frac{1}{16\pi^2}\bigg[-2\eta^3\ln\bigg(\frac{4\eta^2}{\mu^2}\bigg) + 3\eta M^2\ln\bigg(\frac{4\eta^2}{\mu^2}\bigg) \\ &\quad + \frac{3M^4}{4\eta}\ln\bigg(\frac{M^2}{4\eta^2}\bigg) + \ldots\bigg] \\ K_2(\eta, M) &= \frac{1}{16\pi^2}\bigg[-2\eta^3\ln\bigg(\frac{4\eta^2}{\mu^2}\bigg) + \eta M^2\ln\bigg(\frac{4\eta^2}{\mu^2}\bigg) \\ &\quad - \frac{M^4}{4\eta}\ln\bigg(\frac{M^2}{4\eta^2}\bigg) + \ldots\bigg]. \end{aligned} \tag{A4}$$

In these equations we have dropped polynomials of η, M. The functions $K_1(\eta, M)$ and $K_2(\eta, M)$ have well-defined $M \to 0$ limits. Furthermore, the dependence on M is analytic when $M/\eta \to 0$, so in this limit the S fields can be integrated out and their effect on the chiral corrections can be absorbed into local counterterms as expected. This limit is not relevant to the real world as $\eta \sim M$. In the opposite limit, $\eta = 0$, which is relevant for loops in which external and virtual heavy mesons are the same,

$$\begin{aligned} K_1(\eta, M) &= -\frac{M^3}{8\pi} + \frac{3}{16\pi^2}\eta M^2 \ln\left(\frac{4\eta^2}{\mu^2}\right) + O(\eta^3) \\ K_2(\eta, M) &= \frac{1}{16\pi^2}\eta M^2 \ln\left(\frac{4\eta^2}{\mu^2}\right) + O(\eta^3). \end{aligned} \tag{A5}$$

Including the one-loop diagrams we find:

$$\begin{aligned} m_{H_1} = m^0_{H_1} &+ \frac{g^2}{f^2}\left[\frac{3}{2}K_1(m^0_{H_1^*} - m^0_{H_1}, m_\pi) + \frac{1}{6}K_1(m^0_{H_1^*} - m^0_{H_1}, m_\eta) + K_1(m^0_{H_3^*} - m^0_{H_1}, m_K)\right] \\ &+ \frac{h^2}{f^2}\left[\frac{3}{2}K_2(m^0_{S_1} - m^0_{H_1}, m_\pi) + \frac{1}{6}K_2(m^0_{S_1} - m^0_{H_1}, m_\eta) + K_2(m^0_{S_3} - m^0_{H_1}, m_K)\right]. \end{aligned} \tag{A6}$$

$$\begin{aligned} m_{H_3} = m^0_{H_3} &+ \frac{g^2}{f^2}\left[2K_1(m^0_{H_1^*} - m^0_{H_3}, m_K) + \frac{2}{3}K_1(m^0_{H_3^*} - m^0_{H_3}, m_\eta)\right] \\ &+ \frac{h^2}{f^2}\left[2K_2(m^0_{S_1} - m^0_{H_3}, m_K) + \frac{2}{3}K_2(m^0_{S_3} - m^0_{H_3}, m_\eta)\right]. \end{aligned} \tag{A7}$$

$$\begin{aligned} m_{H_1^*} = m^0_{H_1^*} &+ \frac{g^2}{f^2}\frac{1}{3}\left[\frac{3}{2}K_1(m^0_{H_1} - m^0_{H_1^*}, m_\pi) + \frac{1}{6}K_1(m^0_{H_1} - m^0_{H_1^*}, m_\eta) + K_1(m^0_{H_3} - m^0_{H_1^*}, m_K)\right] \\ &+ \frac{g^2}{f^2}\frac{2}{3}\left[\frac{3}{2}K_1(0, m_\pi) + \frac{1}{6}K_1(0, m_\eta) + K_1(m^0_{H_3^*} - m^0_{H_1^*}, m_K)\right] \\ &+ \frac{h^2}{f^2}\left[\frac{3}{2}K_2(m^0_{S_1^*} - m^0_{H_1^*}, m_\pi) + \frac{1}{6}K_2(m^0_{S_1^*} - m^0_{H_1^*}, m_\eta) + K_2(m^0_{S_3^*} - m^0_{H_1^*}, m_K)\right]. \end{aligned} \tag{A8}$$

$$\begin{aligned} m_{H_3^*} = m^0_{H_3^*} &+ \frac{g^2}{f^2}\frac{1}{3}\left[2K_1(m^0_{H_1} - m^0_{H_3^*}, m_K) + \frac{2}{3}K_1(m^0_{H_3} - m^0_{H_3^*}, m_\eta)\right] + \frac{g^2}{f^2}\frac{2}{3}\left[2K_1(m^0_{H_1^*} - m^0_{H_3^*}, m_K) + \frac{2}{3}K_1(0, m_\eta)\right] \\ &+ \frac{h^2}{f^2}\left[2K_2(m^0_{S_1^*} - m^0_{H_3^*}, m_K) + \frac{2}{3}K_2(m^0_{S_3^*} - m^0_{H_3^*}, m_\eta)\right]. \end{aligned} \tag{A9}$$

$$\begin{aligned} m_{S_1} = m^0_{S_1} &+ \frac{g'^2}{f^2}\left[\frac{3}{2}K_1(m^0_{S_1^*} - m^0_{S_1}, m_\pi) + \frac{1}{6}K_1(m^0_{S_1^*} - m^0_{S_1}, m_\eta) + K_1(m^0_{S_3^*} - m^0_{S_1}, m_K)\right] \\ &+ \frac{h^2}{f^2}\left[\frac{3}{2}K_2(m^0_{H_1} - m^0_{S_1}, m_\pi) + \frac{1}{6}K_2(m^0_{H_1} - m^0_{S_1}, m_\eta) + K_2(m^0_{H_3} - m^0_{S_1}, m_K)\right]. \end{aligned} \tag{A10}$$

$$m_{S_3} = m^0_{S_3} + \frac{g'^2}{f^2}\left[2K_1(m^0_{S_1^*} - m^0_{S_3}, m_K) + \frac{2}{3}K_1(m^0_{S_3^*} - m^0_{S_3}, m_\eta)\right] + \frac{h^2}{f^2}\left[2K_2(m^0_{H_1} - m^0_{S_3}, m_K) + \frac{2}{3}K_2(m^0_{H_3} - m^0_{S_3}, m_\eta)\right]. \tag{A11}$$

$$m_{S_1^*} = m^0_{S_1^*} + \frac{g'^2}{f^2}\frac{1}{3}\left[\frac{3}{2}K_1(m^0_{S_1} - m^0_{S_1^*}, m_\pi) + \frac{1}{6}K_1(m^0_{S_1} - m^0_{S_1^*}, m_\eta) + K_1(m^0_{S_3} - m^0_{S_1^*}, m_K)\right] + \frac{g'^2}{f^2}\frac{2}{3}\left[\frac{3}{2}K_1(0, m_\pi) + \frac{1}{6}K_1(0, m_\eta) + K_1(m^0_{S_3^*} - m^0_{S_1^*}, m_K)\right] + \frac{h^2}{f^2}\left[\frac{3}{2}K_2(m^0_{H_1^*} - m^0_{S_1^*}, m_\pi) + \frac{1}{6}K_2(m^0_{H_1^*} - m^0_{S_1^*}, m_\eta) + K_2(m^0_{H_3^*} - m^0_{S_1^*}, m_K)\right]. \quad \text{(A12)}$$

$$m_{S_3^*} = m^0_{S_3^*} + \frac{g'^2}{f^2}\frac{1}{3}\left[2K_1(m^0_{S_1} - m^0_{S_3^*}, m_K) + \frac{2}{3}K_1(m^0_{S_3} - m^0_{S_3^*}, m_\eta)\right] + \frac{g'^2}{f^2}\frac{2}{3}\left[2K_1(m^0_{S_1^*} - m^0_{S_3^*}, m_K) + \frac{2}{3}K_1(0, m_\eta)\right] + \frac{h^2}{f^2}\left[2K_2(m^0_{H_1^*} - m^0_{S_3^*}, m_K) + \frac{2}{3}K_2(m^0_{H_3^*} - m^0_{S_3^*}, m_\eta)\right]. \quad \text{(A13)}$$

We agree with Ref. [38] for the H fields in the limit where $m_\pi \to 0$, $m_\eta^2 \to \frac{4}{3}m_K^2$ and $\eta/M \ll 1$. Our answer also agrees with that of Ref. [45], which computes mass corrections to the H and S masses including $SU(3)$ breaking corrections but not hyperfine splittings.

---

[1] B. Aubert *et al.* (*BABAR* Collaboration), Phys. Rev. Lett. **90**, 242001 (2003).
[2] D. Besson *et al.* (CLEO Collaboration), AIP Conf. Proc. No. 698 (AIP, New York, 2004), p. 497.
[3] S. Anderson *et al.* (CLEO Collaboration), Nucl. Phys. A **663**, 647c (2000).
[4] K. Abe *et al.* (Belle Collaboration), Phys. Rev. D **69**, 112002 (2004).
[5] J. M. Link *et al.* (FOCUS Collaboration), Phys. Lett. B **586**, 11 (2004).
[6] S. Godfrey and N. Isgur, Phys. Rev. D **32**, 189 (1985).
[7] S. Godfrey and R. Kokoski, Phys. Rev. D **43**, 1679 (1991).
[8] J. Hein *et al.*, Phys. Rev. D **62**, 074503 (2000).
[9] P. Boyle (UKQCD Collaboration), Nucl. Phys. B Proc. Suppl. **63**, 314 (1998).
[10] R. Lewis and R. M. Woloshyn, Phys. Rev. D **62**, 114507 (2000).
[11] A. V. Evdokimov *et al.* (SELEX Collaboration), Phys. Rev. Lett. **93**, 242001 (2004).
[12] S. Eidelman *et al.* (Particle Data Group Collaboration), Phys. Lett. B **592**, 1 (2004).
[13] T. Barnes, F. E. Close, and H. J. Lipkin, Phys. Rev. D **68**, 054006 (2003).
[14] S. Nussinov, hep-ph/0306187.
[15] Y. Q. Chen and X. Q. Li, Phys. Rev. Lett. **93**, 232001 (2004).
[16] D. S. Hwang and D. W. Kim, Phys. Lett. B **601**, 137 (2004).
[17] I. W. Lee, T. Lee, D. P. Min, and B. Y. Park, hep-ph/0412210.
[18] Y. A. Simonov and J. A. Tjon, Phys. Rev. D **70**, 114013 (2004).
[19] E. van Beveren and G. Rupp, Phys. Rev. Lett. **91**, 012003 (2003).
[20] E. van Beveren and G. Rupp, Eur. Phys. J. C **32**, 493 (2004).
[21] E. van Beveren and G. Rupp, Phys. Rev. Lett. **93**, 202001 (2004).
[22] E. van Beveren and G. Rupp, Mod. Phys. Lett. A **19**, 1949 (2004).
[23] M. B. Wise, Phys. Rev. D **45**, R2188 (1992); G. Burdman and J. F. Donoghue, Phys. Lett. B **280**, 287 (1992); T. M. Yan, H. Y. Cheng, C. Y. Cheung, G. L. Lin, Y. C. Lin, and H. L. Yu, Phys. Rev. D **46**, 1148 (1992); **55**, 5851(E) (1997).
[24] T. Mehen and R. P. Springer, Phys. Rev. D **70**, 074014 (2004).
[25] P. Colangelo and F. De Fazio, Phys. Lett. B **570**, 180 (2003).
[26] H. Y. Cheng and W. S. Hou, Phys. Lett. B **566**, 193 (2003).
[27] K. Terasaki, Phys. Rev. D **68**, 011501 (2003).
[28] K. Terasaki, AIP Conf. Proc. No. 717 (AIP, New York, 2004), p. 556.
[29] K. Terasaki, hep-ph/0405146.
[30] J. Vijande, F. Fernandez, and A. Valcarce, AIP Conf. Proc. No. 717 (AIP, New York, 2004), p. 352.
[31] P. Colangelo, F. De Fazio, and R. Ferrandes, Mod. Phys. Lett. A **19**, 2083 (2004).
[32] N. Isgur and M. B. Wise, Phys. Lett. B **232**, 113 (1989).
[33] N. Isgur and M. B. Wise, Phys. Lett. B **237**, 527 (1990).
[34] J. L. Rosner and M. B. Wise, Phys. Rev. D **47**, 343 (1993).
[35] L. Randall and E. Sather, Phys. Lett. B **303**, 345 (1993).
[36] N. Di Bartolomeo, R. Gatto, F. Feruglio, and G. Nardulli, Phys. Lett. B **347**, 405 (1995).
[37] B. Blok, J. G. Korner, D. Pirjol, and J. C. Rojas, Nucl. Phys. **B496**, 358 (1997).
[38] E. Jenkins, Nucl. Phys. **B412**, 181 (1994).
[39] T. W. Yeh and C. Lee, hep-ph/9510241.
[40] A. F. Falk and M. E. Luke, Phys. Lett. B **292**, 119 (1992).
[41] W. A. Bardeen and C. T. Hill, Phys. Rev. D **49**, 409 (1994).
[42] W. A. Bardeen, E. J. Eichten, and C. T. Hill, Phys. Rev. D **68**, 054024 (2003).

[43] M. A. Nowak, M. Rho, and I. Zahed, Phys. Rev. D **48**, 4370 (1993).
[44] M. A. Nowak, M. Rho, and I. Zahed, Acta Phys. Pol. B **35**, 2377 (2004).
[45] D. Becirevic, S. Fajfer, and S. Prelovsek, Phys. Lett. B **599**, 55 (2004).
[46] A. F. Falk, Nucl. Phys. **B378**, 79 (1992).
[47] Stephen Wolfram, Mathematica 4.2, Wolfram Research.
[48] F. James, MINUIT, the Function Minimization and Error Analysis program, CERN Program Library entry D506, Geneva, 1994.
[49] I. W. Stewart, Nucl. Phys. **B529**, 62 (1998).
[50] J. Gasser and H. Leutwyler, Nucl. Phys. **B250**, 465 (1985).
[51] S. Ahmed *et al.* (CLEO Collaboration), Phys. Rev. Lett. **87**, 251801 (2001); A. Anastassov *et al.* (CLEO Collaboration), Phys. Rev. D **65**, 032003 (2002).
[52] D. Becirevic and A. L. Yaouanc, J. High Energy Phys. 03 (1999) 021.
[53] C. McNeile, C. Michael, and G. Thompson (UKQCD Collaboration), Phys. Rev. D **70**, 054501 (2004).
[54] A. Abada, D. Becirevic, P. Boucaud, G. Herdoiza, J. P. Leroy, A. Le Yaouanc, and O. Pene, J. High Energy Phys. 02 (2004) 016.
[55] D. Pirjol and T. M. Yan, Phys. Rev. D **56**, 5483 (1997).
[56] A. V. Manohar and M. B. Wise, Cambridge Monogr. Part. Phys. Nucl. Phys. Cosmol. **10**, 1 (2000).
[57] C. W. Bauer, Z. Ligeti, M. Luke, A. V. Manohar, and M. Trott, Phys. Rev. D **70**, 094017 (2004).
[58] A. K. Leibovich, Z. Ligeti, I. W. Stewart, and M. B. Wise, Phys. Rev. D **57**, 308 (1998).